TECHNICAL REPORT ARBRL-TR-02263

MODELING IGNITION AND FLAMESPREAD PHENOMENA IN BAGGED ARTILLERY CHARGES

A. W. Horst
P. S. Gough

September 1980

US ARMY ARMAMENT RESEARCH AND DEVELOPMENT COMMAND
BALLISTIC RESEARCH LABORATORY
ABERDEEN PROVING GROUND, MARYLAND

Destroy this report when it is no longer needed.
Do not return it to the originator.

Secondary distribution of this report by originating or sponsoring activity is prohibited.

Additional copies of this report may be obtained from the National Technical Information Service, U.S. Department of Commerce, Springfield, Virginia 22151.

The findings in this report are not to be construed as an official Department of the Army position, unless so designated by other authorized documents.

The use of trade names or manufacturers' names in this report does not constitute indorsement of any commercial product.

REPORT DOCUMENTATION PAGE

READ INSTRUCTIONS BEFORE COMPLETING FORM

1. REPORT NUMBER: TECHNICAL REPORT ARBRL-TR-02263
2. GOVT ACCESSION NO.:
3. RECIPIENT'S CATALOG NUMBER:

4. TITLE (and Subtitle): MODELING IGNITION AND FLAMESPREAD PHENOMENA IN BAGGED ARTILLERY CHARGES

5. TYPE OF REPORT & PERIOD COVERED: Technical Report

6. PERFORMING ORG. REPORT NUMBER:

7. AUTHOR(s):
A. W. Horst, USA ARRADCOM, BRL, APG, MD
P. S. Gough, Paul Gough Associates, Inc., Portsmouth, NH

8. CONTRACT OR GRANT NUMBER(s):

9. PERFORMING ORGANIZATION NAME AND ADDRESS:
U.S. Army Ballistic Research Laboratory
ATTN: DRDAR-BLP
Aberdeen Proving Ground, MD 21005

10. PROGRAM ELEMENT, PROJECT, TASK AREA & WORK UNIT NUMBERS: 1L161102AH43

11. CONTROLLING OFFICE NAME AND ADDRESS:
U.S. Army Armament Research & Development Command
U.S. Army Ballistic Research Laboratory
ATTN: DRDAR-BL
Aberdeen Proving Ground, MD 21005

12. REPORT DATE: September 1980

13. NUMBER OF PAGES: 44

14. MONITORING AGENCY NAME & ADDRESS (if different from Controlling Office):

15. SECURITY CLASS. (of this report): UNCLASSIFIED

15a. DECLASSIFICATION/DOWNGRADING SCHEDULE:

16. DISTRIBUTION STATEMENT (of this Report)

Approved for public release; distribution unlimited

17. DISTRIBUTION STATEMENT (of the abstract entered in Block 20, if different from Report)

18. SUPPLEMENTARY NOTES

19. KEY WORDS (Continue on reverse side if necessary and identify by block number)
Interior Ballistics
Guns
Flamespreading
Pressure Waves
Computer Codes

20. ABSTRACT (Continue on reverse side if necessary and identify by block number)

jmk

One-dimensional, two-phase flow, interior ballistics codes, successfully applied on numerous occasions to cased-ammunition problems, have proven to be less satisfactory in simulating flamespread and pressurization profiles in bagged propelling charges. Configural complexities associated with the charge/chamber interface, as well as ill-characterized impedances to gas and solid-phase flows offered by the bag and other parasitic components, render treatment of most artillery charges outside the scope of existing models. Simulations of

the US 155-mm, M198 Howitzer firing the Zone 8S, M203 Propelling Charge, obtained using the one-dimensional NOVA code, clarify this problem. Solutions are then presented which are based on a quasi-two-dimensional code in which the charge and the unoccupied portion of the gun chamber are represented as disjoint but coupled regions of one-dimensional flow. Early-time gas flow external to the bag is shown to alter the flame path and equilibrate pressures throughout the chamber; however, this process reflects both the extent and persistence of the ullage, which are seen to be direct consequences of bag dimensions and material characteristics. The impact of these processes on a current effort to develop a fully two-dimensional NOVA code is discussed, and the status of this 2-D code with respect to the bagged-charge problem is outlined.

TABLE OF CONTENTS

LIST OF ILLUSTRATIONS

I. INTRODUCTION

During the past decade, a number of theoretical and experimental efforts have been undertaken to bring about a better understanding of the detailed phenomenology of the gun interior ballistic cycle. A large portion of this work has addressed, in particular, the presence of longitudinal pressure waves in the gun chamber, with practical interest centered on their causes and controls. An extensive review of pressure-wave problems and related propelling charge design considerations was recently provided by May and Horst[1].

The latter half of this same period of time has seen considerable activity in the field of modeling unsteady, multi-phase flows. A small sample of the nature and diversity of such work was revealed at an Army Research Office Workshop on Multi-Phase Flows[2]. One subset in this field has been that of modeling flamespread and combustion in a mobile, granular propellant bed. These studies are of particular interest in terms of their relevance to ignition transients, pressure waves, and even breechblows in artillery and tank guns. The approaches of several flamespread modelers were first reviewed in a JANNAF Workshop[3] several years earlier. Since that time, modeling of flamespread and pressure-wave phenomena has received further attention, primarily by Fisher[4,5],

---

[1] *I.W. May and A.W. Horst, "Charge Design Considerations and Their Effect on Pressure Waves in Guns", Interior Ballistics of Guns, H. Krier and M. Summerfield, Editors, Progress in Astronautics and Aeronautics, Vol. 66, pp. 197-227, AIAA, New York, NY, 1979.*

[2] *J. Chandra and C. Zoltani, Editors, Proceedings of ARO Workshop on Multiphase Flows, US Army Research Office, Research Triangle Park, NC, February 1978.*

[3] *K.K. Kuo, "A Summary of the JANNAF Workshop on Theoretical Modeling and Experimental Measurements on the Combustion and Fluid Flow Processes in Gun Propellant Charges", 13th JANNAF Combustion Meeting, CPIA Publication 281, pp. 213-234, December 1976.*

[4] *E.B. Fisher, "Quality Control of Continuously Produced Gun Propellant", Calspan Report No. SA-5913-X-1, Calspan Corporation, Buffalo, NY, August 1977.*

[5] *E.B. Fisher, "Investigation of Breechblow Phenomenology", Calspan Report No. 1359-D-1, Calspan Corporation, Buffalo, NY, April 1979.*

Gough[6,7,8], and Kuo[9]. Other modeling efforts recently sponsored by the US Army[10,11] are addressing post-flamespread phenomena and, hence, are not relevant to the description of ignition/combustion-driven pressure waves.

Both because pressure waves in guns are a largely one-dimensional phenomenon and because it represented a logical first step in modeling, nearly all of the emphasis was initially placed on providing a digital simulation of flamespread and pressure waves within the limitation of a one-dimensional representation. This approximation was considered reasonable for a number of applications of interest involving base ignition of a bed of radially-confined propellant. As our present understanding of pressure waves in guns associates their formation with an axially localized ignition stimulus, an axially nonuniform distribution of propellant, or perhaps an interaction between these inhomogeneities, the one-dimensional treatment can be seen to have been physically well motivated.

Indeed, application of at least one of these codes to radially-confined charges (e.g., cased ammunition) met with success on numerous

---

[6] *P.S. Gough and F.J. Zwarts, "Some Fundamental Aspects of the Digital Simulation of Convective Burning in Porous Beds", AIAA Paper No. 77-855, AIAA/SAE 13th Propulsion Conference, July 1977.*

[7] *P.S. Gough, "Theoretical Study of Two-Phase Flow Associated with Granular Bag Charges", ARBRL-CR-00381, USA ARRADCOM, Ballistic Research Laboratory, Aberdeen Proving Ground, MD, September 1978.* (AD#A062144)

[8] *P.S. Gough, "Two Dimensional Convective Flamespreading in Packed Beds of Granular Propellant", ARBRL-CR-00404, USA ARRADCOM, Ballistic Research Laboratory, Aberdeen Proving Ground, MD, July 1979.* (AD#A075326)

[9] *K.K. Kuo and J.H. Koo, "Transient Combustion in Granular Propellant Beds. Part 1: Theoretical Modeling and Numerical Solution of Transient Combustion Processes in Mobile Granular Propellant Beds", BRL-CR-346, USA ARRADCOM, Ballistic Research Laboratory, Aberdeen Proving Ground, MD, August 1977.* (AD#A044998)

[10] *H. McDonald, "Two-Dimensional Implicit Interior Ballistics Code-Quarterly Technical Progress Report", Scientific Research Associates, Inc., November 1978.*

[11] *A.C. Buckingham, "Research on Gun Barrel Erosion Mechanisms", Energy and Technology Review, Lawrence Livermore Laboratory, CA, January 1979.*

occasions[12,13]; however, similar levels of success were not forthcoming with bagged-charge configurations[14,15]. This problem was recognized by Fisher[16] and subsequently by Gough[7], both of whom suggested that for bagged charges with annular ullage external to the propellant package present, a high permeability path may be provided for equilibration of pressure gradients early in the ballistic cycle. Conversely, the presence of the bag material itself, as well as other parasitic components such as wear-reducing liners, may alter flamespread and decrease overall permeability of the charge.

In this report, simulations of a bagged charge are provided based on two alternative representations: first, a one-dimensional-with-area-change treatment which assumes a uniform cross-sectional distribution of propellant (if present) at any given axial location; and second, a quasi-two-dimensional analysis which treats the propelling charge and unoccupied regions in the gun chamber as disjoint but coupled regions of one-dimensional flow. With the latter, some aspects of charge geometry, ullage, and bag material characteristics are amenable to investigation for possible effects on flamespread and pressure waves.

Finally, a technical approach for a fully two-dimensional treatment of the problem is described.

II. TECHNICAL DISCUSSION

A. Description of the Problem

The M203 Propelling Charge is a conventional, top-zone, bagged charge, recently released for use in the M198 Towed Howitzer and currently

---

[12] *A.W. Horst, T.C. Smith, and S.E. Mitchell, "Key Design Parameters in Controlling Gun-Environment Pressure Wave Phenomena - Theory Versus Experiment", 13th JANNAF Combustion Meeting, CPIA Publication 273, pp. 341-368, December 1975.*

[13] *A.W. Horst and P.S. Gough, "Influence of Propellant Packaging on Performance of Navy Case Gun Ammunition", Journal of Ballistics, Vol. 1, No. 3, pp. 229-258, 1977.*

[14] *C.W. Nelson, "Comparison of Predictions of Three Two-Phase Flow Codes", BRL-MR-2729, USA ARRADCOM, Ballistic Research Laboratory, Aberdeen Proving Ground, MD, February 1977.* (AD#A037348)

[15] *A.W. Horst, C.W. Nelson, and I.W. May, "Flame Spreading in Granular Propellant Beds: A Diagnostic Comparison of Theory to Experiment", AIAA Paper No. 77-856, AIAA/SAE 13th Propulsion Conference, July 1977.*

[16] *E.B. Fisher and A.P. Trippe, "Development of a Basis for Acceptance of Continuously Produced Propellant", Calspan Report No. VQ-5163-D-1, Calspan Corporation, Buffalo, NY, November 1973.*

undergoing evaluation in the M109A2/A3 Self-Propelled Howitzer. Depicted in Figure 1, this charge employs about 11.8 kg of M30A1, triple-base, granular propellant. The ignition system is comprised of a cloth basepad containing 28 g of Class 1 black powder and a molded-nitrocellulose centercore tube, which houses a cloth snake filled with an additional 113 g of black powder. The charge, confined within a resin-impregnated cloth bag, is encumbered with a number of parasitic components, each designed to perform a special function. A cloth donut filled with granular potassium sulfate serves to reduce muzzle flash. Lead foil, a de-coppering agent, and a titanium-dioxide/wax wear-reducing additive are also present as liners which surround approximately the forward two-thirds of the charge. Finally, a cloth lacing jacket provides additional rigidity to the package.

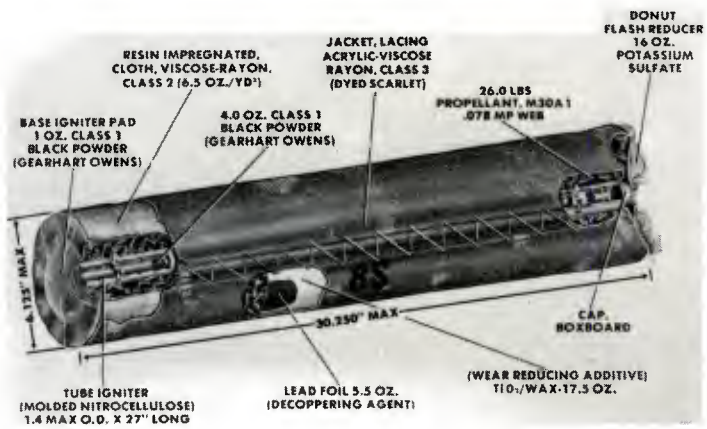

Figure 1. 155-mm, M203 Propelling Charge

The impact of these various components on the details of the early portion of the interior ballistic cycle is unknown. Nevertheless, it is readily apparent that a potential exists for these elements to affect not only the early-time flow of igniter gases into and around the propellant bed, but also to restrict or alter mobility of the solid propellant itself.

Consider what is believed to be the normal sequence of events during functioning of this charge. Hot combustion products from the primer exit the spithole in the spindle face and impinge upon the basepad*. As the

* *While the details of this process are outside the scope of the present study, an approach for modeling the M82 Primer has been provided by Zoltani.*[17]

[17] *C.K. Zoltani, "M-82 Primer Flow Study", ARBRL-TR-02084, USA ARRADCOM, Ballistic Research Laboratory, Aberdeen Proving Ground, MD, June 1978.* (AD#A057695)

basepad begins to burn, product gases and hot particles will penetrate the several layers of cloth, enter the centercore tube, and ignite the snake as intended. However, basepad combustion products will also tend to penetrate the rear of the bag and ignite the main propellant charge directly. This competition with centercore functioning is critical, and a victory for direct, local ignition of the propellant bed by the basepad could lead to catastrophic pressure waves in a high-loading-density charge. Basepad products, however, can also flow into axial ullage behind the charge and forward, external to the bag, via annular ullage shown in Figure 2. Such flow around the bag could equilibrate pressures throughout the chamber early in the cycle, but the persistance of this ullage is unknown and may depend heavily on charge-component characteristics. Figure 2 also indicates extreme loading positions for the M203 in the M198 Howitzer. The variation in charge standoff from the spindle face can be expected to affect coupling between primer spithole output and the basepad, as well as alter the initial distribution of propellant and ullage.

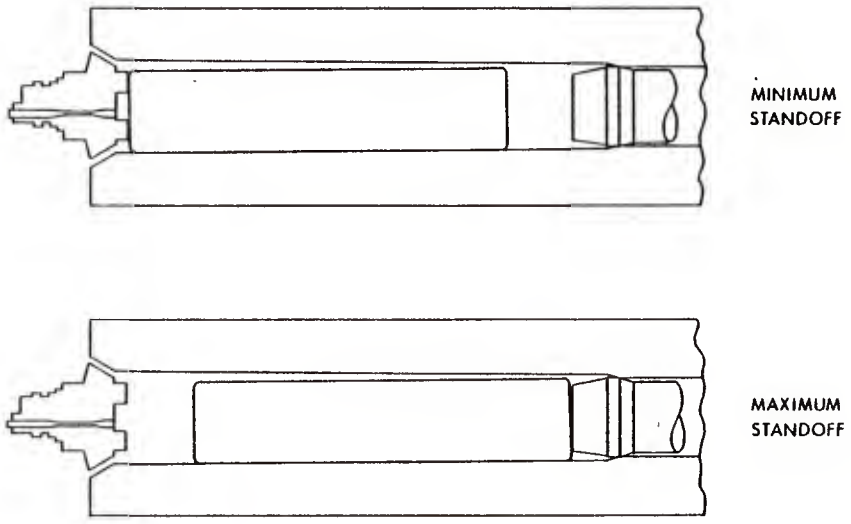

Figure 2. Extreme Loading Positions of the M203 Propelling Charge in the M198 Howitzer

Thus, we have identified unintended contributors to mechanisms both for localizing ignition and pressurization and for preventing or reducing longitudinal pressure gradients. In this study, we address three of these factors - distribution of ullage, permeability of the bag sidewall, and rupture strength of the bag - to assess their influence on the flow of igniter gases and on the subsequent processes of flamespread and pressurization.

B. Quasi-One-Dimensional Treatment

Several versions of the NOVA code have been generated since its birth in 1972. Documentation on the most recent NOVA code is undergoing preparation by Paul Gough Associates and will be published as a Naval Ordnance Station, Indian Head (NOS/IH) Contract Report. A recent AIAA publication[6] provides an essentially accurate description of this code as used in the current study.

NOVA consists of a two-phase flow treatment of the gun interior ballistic cycle formulated under the assumption of quasi-one-dimensional flow. The balance equations describe the evolution of averages of flow properties accompanying changes in mass, momentum, and energy arising out of interactions associated with combustion, interphase drag, and heat transfer. Constitutive laws include a covolume equation of state for the gas and an incompressible solid phase. Compaction of an aggregate of grains, however, is allowed, with granular stresses in excess of ambient gas pressure taken to be dependent on porosity and in accord with steady state measurements. Interphase drag is represented by reference to the empirical, steady state correlations of Ergun[18] and Anderson[19] for fixed and fluidized beds, respectively. Interphase heat transfer is described similarly according to Denton[20] or Gelperin-Einstein[21]. Functioning of the igniter is included by specifying a predetermined mass injection rate as a function of position and time. Flamespreading then follows from axial convection, with grain surface temperature deduced from the heat transfer correlation and the unsteady, heat conduction equation, and ignition based on a surface temperature criterion. In addition, internal boundaries defined by discontinuities in porosity are treated explicity, and a lumped-parameter treatment is included reflecting the inertial and compactibility characteristics of any inert packaging elements present between the propellant bed and the base of the projectile. Solutions are obtained using an explicit finite difference scheme based on the method of MacCormack[22] for points

[18] *S. Ergun, "Fluid Flow Through Packed Columns", Chem. Eng. Progr., Vol 48, pp. 89-95, 1952.*

[19] *K.E.B. Anderson, "Pressure Drop in Ideal Fluidization", Chem. Eng. Sci., Vol. 15, pp. 276-297, 1961.*

[20] *W.H. Denton, "General Discussion on Heat Transfer", Inst. Mech Eng. and Am. Soc. Mech. Eng., London, 1951.*

[21] *N.I. Gelperin and V.G. Einstein, "Heat Transfer in Fluidized Beds", Fluidization, J.F. Davidson and D. Harrison, Editors, Academic Press, 1971.*

[22] *R.W. MacCormack, "The Effects of Viscosity in Hypervelocity Impact Cratering", AIAA Paper No. 69-354, AIAA 7th Aerospace Science Meeting, 1969.*

in the interior and a modified method of characteristics at internal and external boundaries. The configural approximation imposed by this representation is schematically depicted in Figure 3.

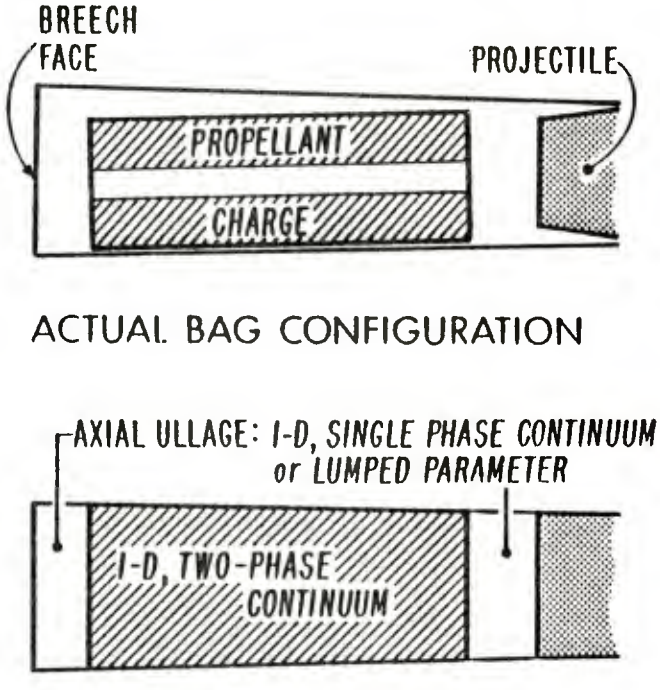

Figure 3. Actual Charge/Chamber Interface and Quasi-One-Dimensional Representation

C. Quasi-Two-Dimensional Treatment

As with the quasi-one-dimensional model, the quasi-two-dimensional model has already been documented elsewhere in many essential respects[7]. We therefore confine our present discussion to a summary of the overall physical features and comment in detail only on those features which differ from our earlier work.

The quasi-two-dimensional treatment involves the decomposition of the combustion chamber into four distinct regions: namely, the contents of the bag, the ullage to the rear of the bag, the ullage to the front of the bag and, lastly, the ullage around the bag. We find it convenient to refer to the ullage at the rear and front of the charge as axial ullage and to refer to that which surrounds the bag as annular ullage (see Figure 4). Evidently, only the axial ullage is recognized explicitly by the quasi-one-dimensional treatment. The significant features of the quasi-two-dimensional treatment are (1) the explicit recognition of annular ullage and the influence of the strength and permeability

of the bag sidewall on the radial motion of the charge, and (2) the exchange of mass between the charge and the annular ullage.

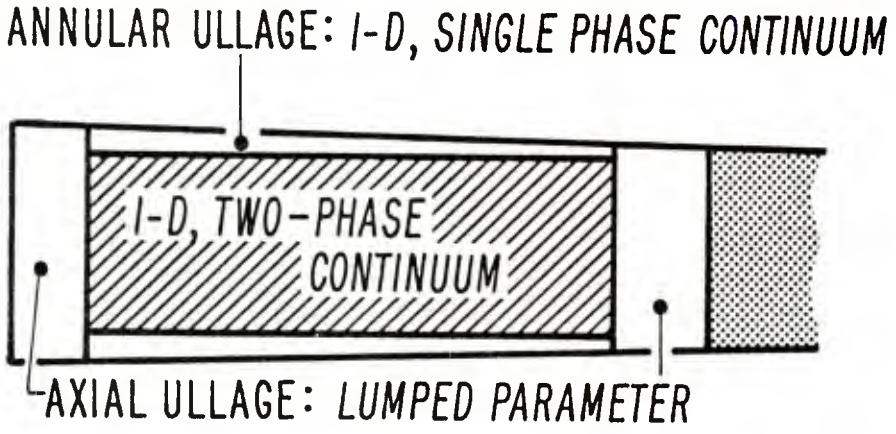

Figure 4. Quasi-Two-Dimensional Representation of Charge/Chamber Interface

The model for the two-phase flow within the bag differs from that summarized in the preceding section only by virtue of the time-dependent cross-sectional area for the flow which is a consequence of radial motion of the boundary between the propellant and annular ullage and the influence of radial mass transfer. Our earlier account[7] may be consulted for further details. The current treatment also follows our earlier approach in regard to the analysis of ullage. The annular ullage is represented as a quasi-one-dimensional, single-phase inviscid flow. The time dependence of the local cross section is, of course, recognized. The axial ullage is, however, always treated according to a lumped-parameter representation. A more detailed representation is not thought to be justified in view of the quasi-one-dimensional treatments of the bag and annular ullage. Indeed, an attempt to represent more fully the details of the flow in the axial ullage would virtually demand a fully two-dimensional analysis as the circulation in these regions is expected to be intense.

The essentially new details of the present treatment relate to the representation of the characteristics of the bag material. The bag is assumed to be characterized initially by a rupture strength, σ_{bag}, which is a function of position. Also, the bag is regarded as either fully permeable (to the gas phase) or fully impermeable at any time. The local permeability can be initialized as either "go" or "no-go". When rupture is detected, the local permeability automatically defaults to a "go" condition. Radial elasticity of the bag is not considered; the bag

is assumed to be incapable of dilation beyond its initial diameter except as a consequence of rupture. The behavior of the bag following local rupture is not considered.

The rupture condition recognizes the contributions of granular stress and of the differential in gas pressure if the bag is impermeable. As in the previous study[7], we assume the granular stress to be hydrostatic. This has the consequence of imposing a local condition of radial equilibrium in the sense that the granular stress must vanish unless there is suitable radial confinement. Full confinement is provided, of course, when the charge is in contact with the wall of the tube and, also, when the unruptured bag is fully dilated to its initial diameter. When the bag is ruptured, the granular stress must vanish locally until such time as contact with the wall occurs. Similarly, if the impermeable bag is not fully dilated, the granular stress must be equal in value to the excess of the external pressure over the internal pressure, provided this is positive. These principles of radial equilibrium provide important mechanisms for the radial motion of the boundary between propellant and annular ullage since adjustments in granular stress require adjustments in porosity, which in turn influence the local diameter.

In addition to radial motion due to stress equilibration, we consider the influence of the radial component of drag due to mass transfer. The approach to this detail has been given previously[7].

In the present group of calculations, we have considered the effects of radial drag and stress relaxation to be linearly additive over each time step in accordance with the following basic algorithm. Based on the local permeability, we compute the mass transfer, the induced drag, the resulting change in radial velocity, and the change in local cross-sectional area due to expansion. Subsequently, within each integration step, the constraints imposed by considerations of radial equilibrium are taken into account. If the charge is unconfined and the computed change in cross-sectional area has led to a non-zero value of granular stress, the area is adjusted locally so as to relax the stress to zero by a suitable variation in the porosity. A similar procedure is applied to ensure the equilibration of pressure excess on an impermeable bag by granular stress within the bag.

We conclude by noting some of the possible aspects of bag behavior which have not been addressed by the present study. These include ablation or thermal and erosive destruction of the bag; influence of the ruptured bag on subsequent processes; dilation of the unruptured bag and separation from grains under internal pressure excess; details of the axial motion of the bag or end effects such as grain spillout; and any details of the end closures, which are always taken as fully permeable.

III. RESULTS OF CALCULATIONS

A. Quasi-One-Dimensional Solutions

A complete listing of all input data used to perform the quasi-one-dimensional simulations is provided as Appendix A. Further discussion of these data and a description of results for a nearly identical problem have been provided previously by Horst and Trafton[23]. The problem reported herein differs only in initial charge length and details of the chamber geometry.

We comment first on the fact that while experimentally observed muzzle velocities and, to a lesser degree, maximum chamber pressures are usually quite reproducible, the presence of longitudinal pressure waves may pass all but unnoticed or be quite pronounced. Smooth pressurization profiles are usually associated with proper and prompt initiation of the centercore black powder charge, which in turn ignites the main propellant charge over a distributed longitudinal region in an effectively simultaneous time frame. On the other hand, late initiation of the centercore, perhaps resulting from misalignment between the spindle spithole and the centercore, might lead to direct ignition transfer from the basepad to the main propellant charge - a more localized ignition, favoring the formation of pressure waves. It is also important to note that ignition delays for ambient ($\sim$ 21°C) firings usually fall in the 50-100 ms range, a figure an order of magnitude higher than that typically exhibited by cased charges employing high-pressure bayonet primers.

A quasi-one-dimensional NOVA code simulation of the M203 Charge, properly loaded in the gun chamber with the basepad approximately 25 mm from the spindle face, provided the results depicted in Figure 5. Overall pressurization profiles are quite similar to experimental data. Detailed analysis of a comparison of predicted and observed pressure-difference profiles, however, reveals some disturbing features (see Figure 6). First, we notice a strong, predicted positive difference (i.e., local pressurization at the breech end of the chamber) not observed experimentally. This prediction is a consequence of the one-dimensional approximation, which requires that all basepad combustion products pass into the low permeability propellant bed, as opposed to venting around the charge external to the bag, rapidly equilibrating pressures throughout the chamber. The schematic representations of Figure 3 serve to clarify this point. This same configural difference between NOVA and reality may also be responsible, in part, for the predicted, short ignition delays ($\sim$ 5 ms). Additional major contributions to the real-world delay ($\sim$ 60 ms) may be associated with the impedance to flame penetration offered by the bag and other parasitic components themselves.

---

[23] *A.W. Horst and T.R. Trafton, "NOVA Code Simulation of a 155-mm Howitzer: An Update", ARBRL-MR-02967, USA ARRADCOM, Ballistic Research Laboratory, Aberdeen Proving Ground, MD, October 1979.* (AD#A079893)

As a result of the predicted, rapid ignition at the rear of the main charge, input data reflecting functioning of the igniter centercore are of no consequence, as they represent igniter output after flamespread throughout the bed has been calculated to be complete. Hence, NOVA predicts a monotonic propagation of flame forward through the bed, accompanied by a strong stagnation at the projectile base (indicated in Figure 5 by an initial reverse pressure difference of $\sim$ 20 MPa). However, the resulting longitudinal pressure wave is predicted to decrease rapidly in amplitude. An experimental curve exhibiting a similar initial reverse pressure-difference level (which contributed to Figure 6) does not reveal the same characteristic damping rate. This discrepancy may reflect some inadequcy of the interphase drag law included in NOVA, coupled perhaps with a misrepresentation of propellant bed rheology - neither element of constitutive physics being adequately supported by experimental data.

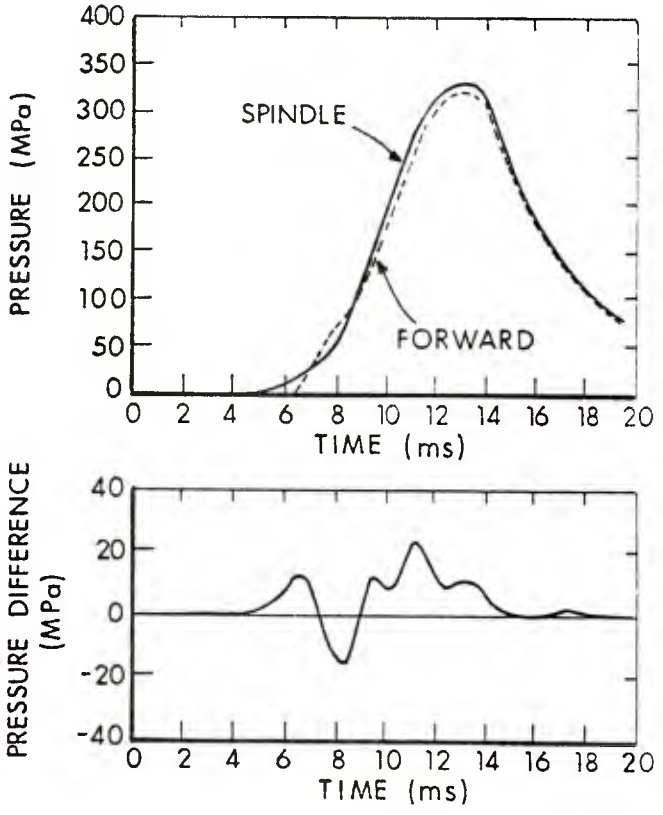

Figure 5. NOVA Simulation: M203 Propelling Charge, 25-mm Standoff

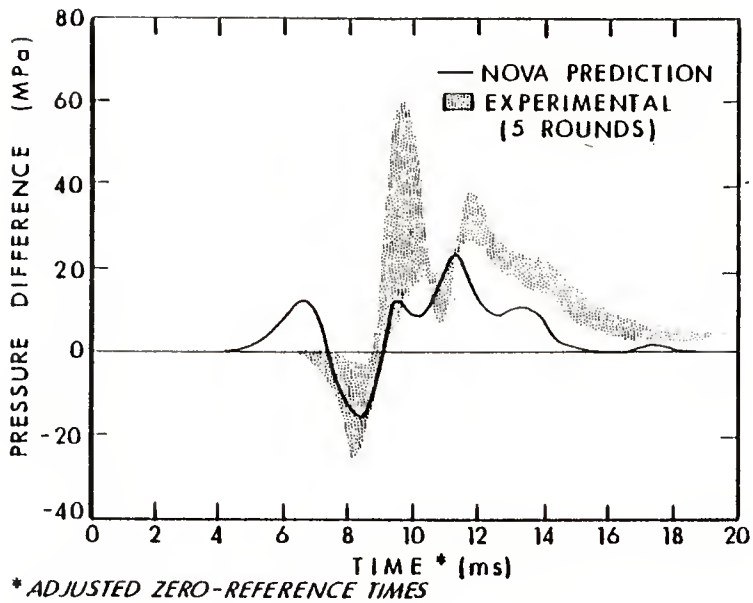

Figure 6. Comparison of NOVA Simulation to Experimental Pressure-Difference Profiles: M203 Propelling Charge, 25-mm Standoff

A NOVA calculation was also performed to simulate the loading condition whereby the propelling charge is pushed all the way forward against the projectile base. With the M483A1 Projectile and the M203 Propelling Charge, this configuration may result in as much as 130 mm between the spindle face and the base of the charge. With the exception of this initial positioning of the charge, input data remained the same as for the previous problem. Figure 7 presents pressurization profiles resulting from this calculation which indicate an increased level of longitudinal pressure waves. The predicted pressure-difference profile is compared to a band of maximum-standoff, firing data in Figure 8. We see excellent qualitative and fairly good quantitative agreement between theory and experiment. As before, the predicted pressure waves tend to dampen out more rapidly than is indicated by the firing data. Of more concern, however, is the continued disparity between NOVA and reality prior to completion of flamespread and the initial stagnation at the projectile base. We still observe an order-of-magnitude difference in ignition delays between experiment and theory (not obvious in the figures because zero reference times were shifted when presenting experimental data).

The one-dimensional approximation does appear, however, to have provided a much more satisfactory simulation of the maximum charge standoff configuration than of the nominal 25-mm condition. At this point, the improvement may be considered to result chiefly from an

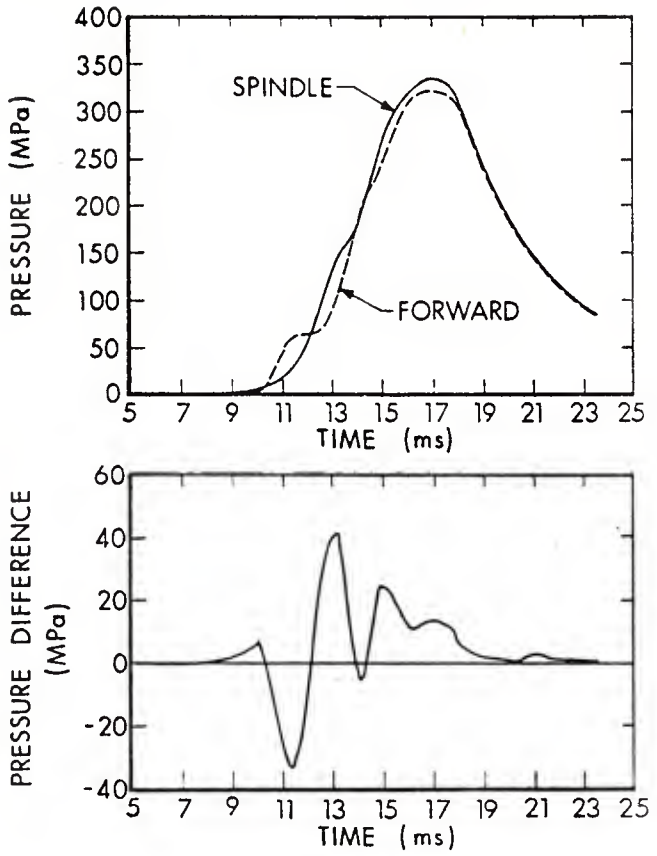

Figure 7. NOVA Simulation: M203 Propelling Charge, Maximum Standoff

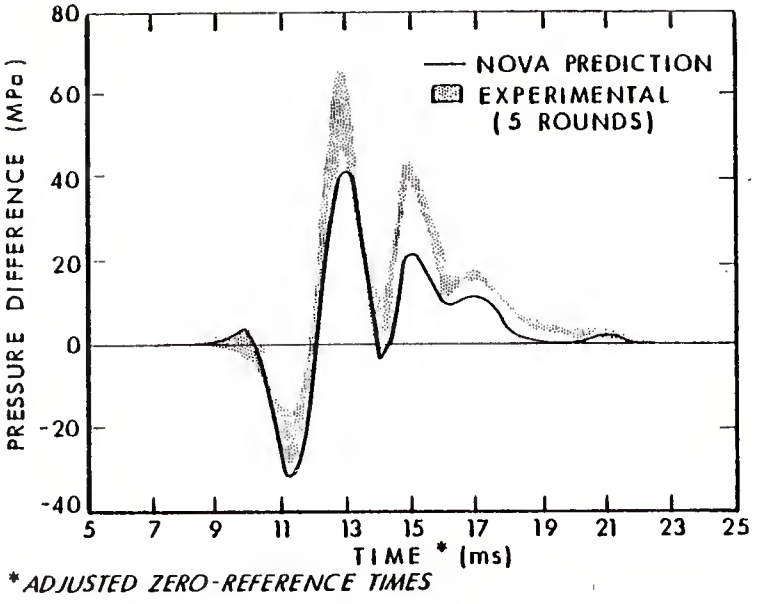

Figure 8. Comparison of NOVA Simulation to Experimental Pressure-Difference Profiles: M203 Propelling Charge, Maximum Standoff

increased likelihood of largely base ignition of the main charge at maximum standoff, a consequence of the poorer interface between the primer spithole and the igniter centercore charge. Coupled with a slight reduction in annular ullage external to the charge (because of the tapered gun chamber) and elimination of the forward reservoir of ullage, this mode of ignition may lead to a nearly one-dimensional process (at least on the macroscopic level), more successfully represented in NOVA. Predicted flame propagation through the charge, shown in Figure 9, is essentially equivalent for the two configurations, except for initial ignition delays.

B. Quasi-Two-Dimensional Solutions

The input data for the quasi-two-dimensional calculations differed from those for the one-dimensional treatment only in that entries were included to represent explicitly the propellant as being confined in a bag characterized by initial radius, rupture strength, and permeability. Treatment of the behavior and influence of the bag was described previously; it is re-emphasized here that this picture grossly oversimplifies reality. Nevertheless, we hoped to provide information on several limiting cases which together would increase our insight into the influence of real propellant bags on the evolution of the interior ballistics cycle, as well as to probe the potential importance of bag materials and configuration as available propelling charge design parameters.

Toward this end, calculations were performed for charges with three different "limiting-case" bag materials, each at both minimum and maximum standoff distances from the spindle face. Input data are summarized as Appendix B.

The first of these was designated the weak, permeable bag. In the spirit of providing a bound on reality, the bag was taken to have no strength and to provide no resistance to gas flow. Thus, the bag served only to describe an initial boundary between the propellant bed and external ullage, offering no further constraint on the problem. In the calculation, igniter gases are initially predicted to flow around the charge as well as into the base of the propellant bed. This leads to a reversal of flow at the front of the chamber and some local preheating of the forward end of the propellant bed. Histories of flamespreading for this and one other quasi-two-dimensional simulation of a minimum standoff configuration, shown as a portion of Figure 10, reflect increased flamespreading rates in this region when compared to the NOVA predictions of Figure 9 - the difference primarily a result of this preheating.

Very early in the cycle, however, local ignition and pressurization at the rear of the charge result in expansion of the propellant bed to the chamber wall at the two rear-most axial stations. Pressurization of the rear ullage also moves the rear boundary of the charge forward, with the reshaped, rear portion of the bed maintaining porosity levels very near to settling. Limitations imposed by the code necessitate

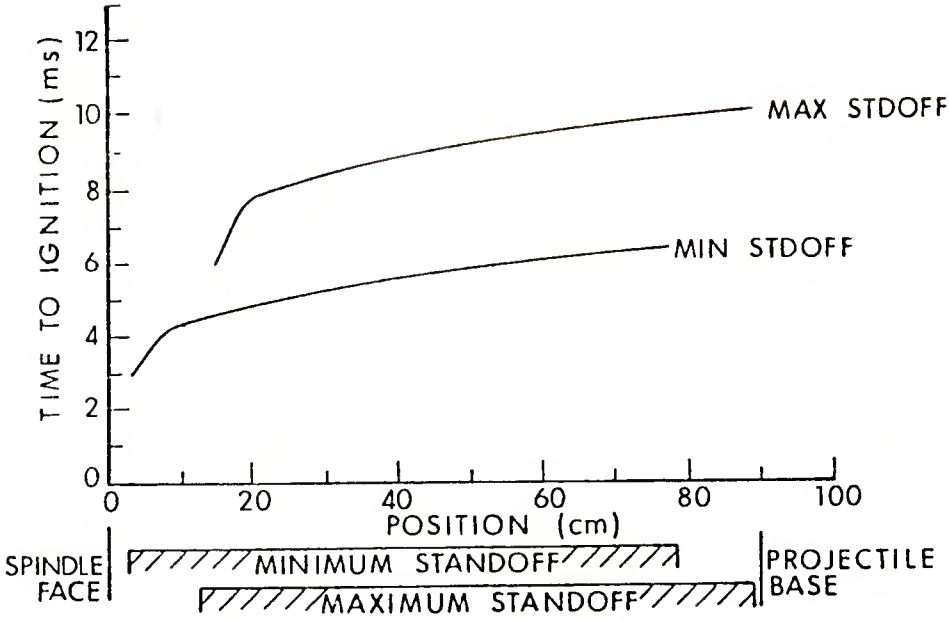

Figure 9. NOVA Predictions of Flamespread

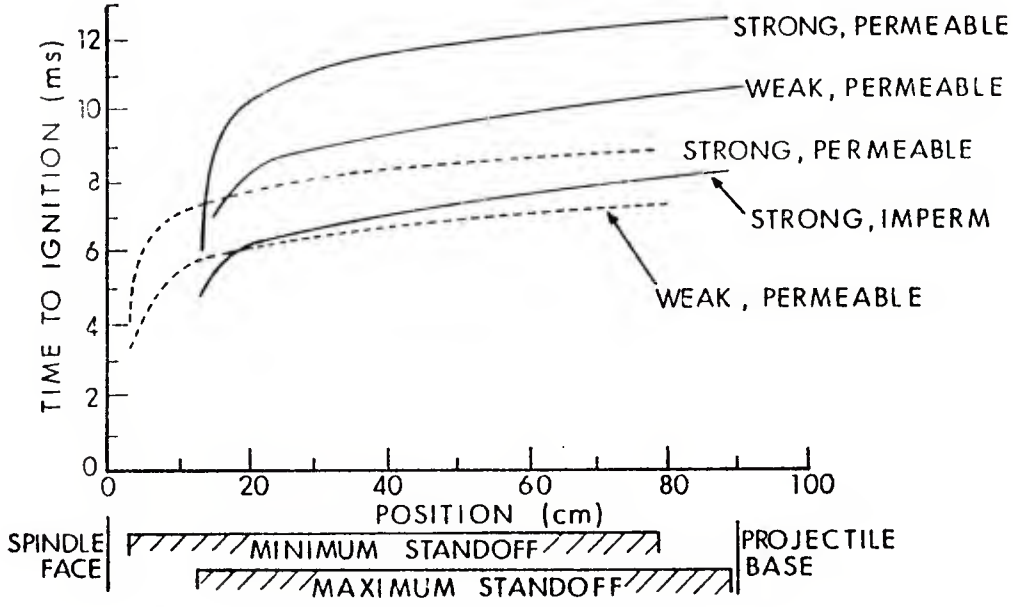

Figure 10. Quasi-Two-Dimensional Predictions of Flamespread

defaulting to the quasi-one-dimensional representation at this point. The inability to continue the quasi-two-dimensional treatment further, though certainly undesired, is not believed to discredit the calculation beyond interest, since contact of the charge against the chamber wall effectively ends communication between the two ends of the chamber via the high-permeability, annular ullage. Conversion to the quasi-one-dimensional representation does, however, lead to a large difference (10-15%) in propellant bed porosity between previously expanded and unexpanded bag stations, as well as a moderate, negative porosity gradient as one moves forward through the previously unexpanded portion. Thus, despite the fact that nearly all the flamespreading is then calculated using the same representation that led to the NOVA solution discussed earlier, a significantly different result is provided. The locally lower porosities at the rear of the charge apparently impede escape of early combustion products, yielding an increased level of pressurization at the breech end of the chamber, as shown by the appropriate curve of Figure 11. The convectively driven flame front then propagates through the charge, encountering an ever-decreasing bed permeability. The pressure front is "focussed" by the continually increasing resistance to flow, resulting in a vigorous stagnation event at the projectile base and local pressures exceeding even those exhibited in the one-dimensional NOVA simulation.

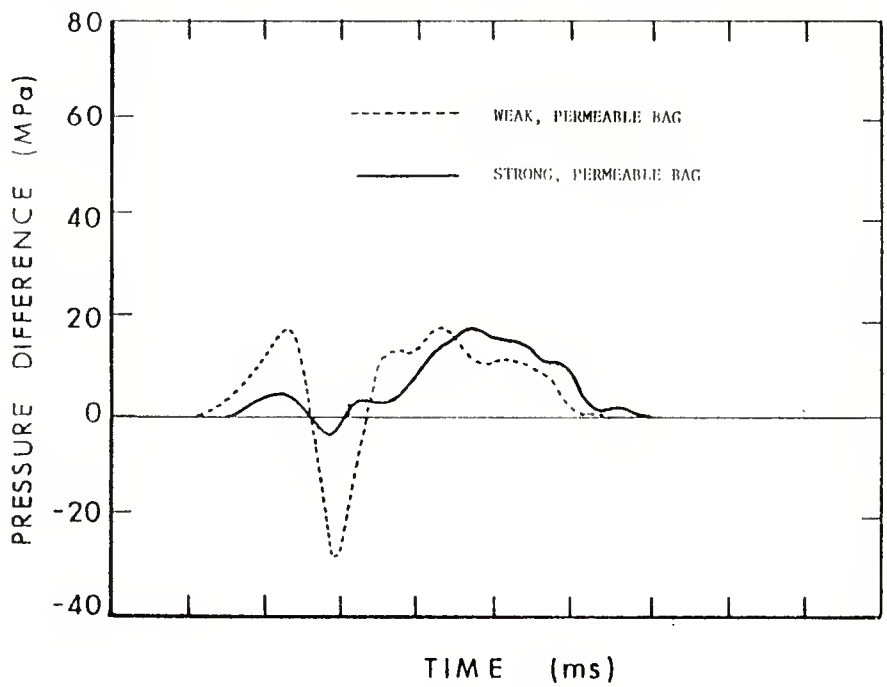

Figure 11. Quasi-Two-Dimensional Predictions of Pressure-Difference Profiles for Minimum-Standoff Conditions

In a similar fashion, simulation of the maximum-standoff, weak, permeable bag leads to an early (t - $\sim$ 5 ms) collapse of the bag sidewall against the chamber, necessitating a default to the one-dimensional representation for the remainder of the calculation. However, Figures 10 and 12 reveal little difference from the one-dimensional NOVA solution for this configuration.

A second, though unlikely, bound on reality was supplied in the form of a strong, impermeable bag, capable of withstanding the entire interior ballistic cycle without rupture while allowing combustion products to exit via the ends of the charge only. Interestingly enough, the minimum- standoff calculation does not lead to propellant ignition. Virtually all of the igniter gases are bled off around the charge to the forward, axial ullage, while little of the gases penetrate the comparatively impermeable, confined bed to heat the propellant. Figure 13 provides a display of the bed temperature profile at the time of maximum temperature at the first station. To probe this result further, an additional calculation was performed with the igniter output profile doubled over the same time interval. We see propellant ignition to occur at about only 3.5 ms into the cycle, revealing the sensitivity of our ignition limit to igniter characterization, an area certainly worthy of further experimental work. Even more interesting is the bed temperature profile several milliseconds later, when flow of combustion products around the bag leads to reversed flow, actually creating a second ignition site at the forward end of the bed. A similar calculation, leading to the coalescence of the two flames inside the bed and a reduced level of pressure waves, has been previously described by Gough[7].

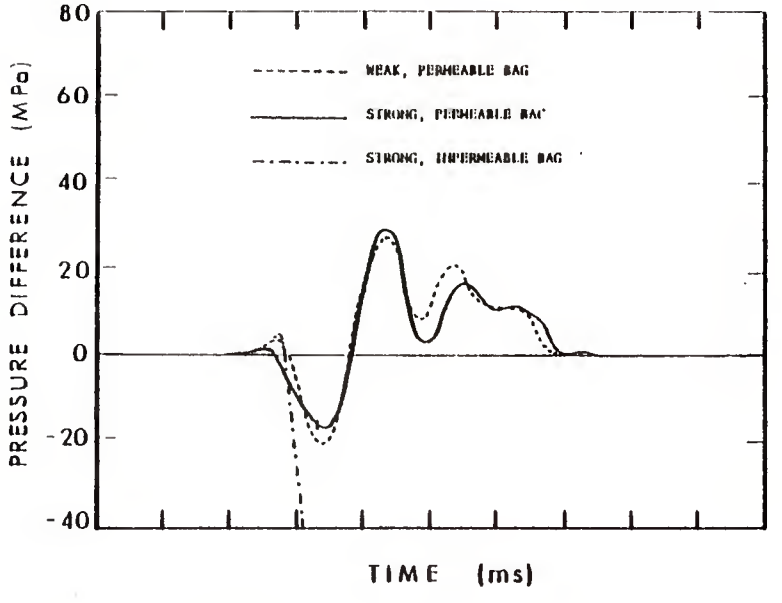

Figure 12. Quasi-Two-Dimensional Predictions of Pressure-Difference Profiles for Maximum-Standoff Configurations

Simulation of the strong, impermeable bag in the maximum standoff loading condition provides a dramatic, though not altogether unexpected, result. Ignition is not abated by the strong confinement of the bed and persistent annular ullage, apparently because of the limits on loss of igniter products around the bag without a forward region of ullage present. However, the infinitely strong bag, because of its condition of total sidewall impermeability, acts much like a gun chamber of reduced diameter. Stagnation of the initial pressurization front at the base of the projectile results in extreme compaction of the bed (porosity $\simeq$ 0.27) and a violently high, local pressurization rate, as indicated in Figure 12. The computational scheme employed in the code was taxed at this point, and the calculation was terminated for reasons of economy.

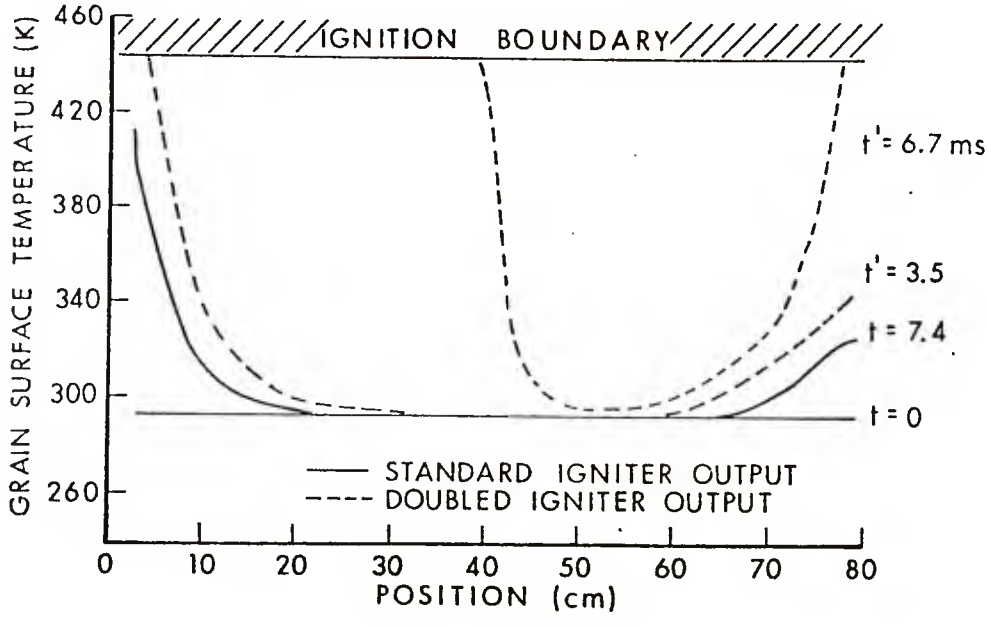

Figure 13. Propellant Bed Heating Profiles: Minimum Standoff; Strong, Impermeable Bag

A final configuration included in this study was that of a strong permeable bag. Again, the bag was taken to have whatever characteristics of durability that were necessary to survive the interior ballistic cycle, but this time the sidewall as well as the ends were taken to be totally permeable to gas flow. Since only intergranular stresses had to be supported by the sidewall, this requirement on strength was less severe than that for the impermeable case. The results of calculations for both minimum and maximum standoff conditions are summarized graphically again in Figures 10 through 12. Unlike the impermeable bag simulation indicating non-ignition at minimum standoff, an apparent

venturi effect encourages igniter gases to enter the bed and immediately exit through the permeable sidewall to the lower pressure region of annular ullage. As a result of this same process, direct loss of igniter products from the rear region of axial ullage through the annulus is reduced. Convective input to the first station of propellant is increased and ignition results. A large period of hesitation, however, is then seen for both minimum and maximum standoffs, as any local pressurization capable of driving the convective flame into the bed is also depleted by flow around and through the permeable sidewall. Nevertheless, once the flame is sufficiently fed by propellant combustion, flamespreading rates are predicted to be similar to those provided by the one-dimensional NOVA simulations.

These same configural factors - sidewall permeability and persistent annular ullage - can significantly alter the development of pressure gradients leading to longitudinal pressure waves. In the minimum-standoff simulation, local pressurization at the breech end of the chamber accompanying propellant ignition is drastically reduced, all but eliminating subsequent development of a longitudinal pressure wave. Igniter gases and propellant combustion products are free to propagate throughout the annular ullage, reaching the forward axial ullage and essentially equilibrating pressures throughout the chamber as long as this highly permeable path remains open.

Initial reductions in breech pressurization mitigate the formation of gas-phase pressure waves, which in turn reduces motion of the propellant, stagnation of which against the projectile base can further increase local gas pressures. The situation may be even worse than the simulations relate, as impact of propellant grains into the projectile base may lead to grain fracture, a mechanism implicated in breechblows[24].

A simulation of the maximum-standoff loading condition, however, indicates a significantly reduced impact of annular ullage on the development of pressure waves. While Figure 12 reveals minor differences in the character of the pressure-difference profile from the other maximum-standoff configurations, the amplitudes of minima and maxima are essentially unchanged. The lack of a receiving reservoir in the form of forward axial ullage appears to be a key factor in desensitizing the charge to bag properties when fired at maximum standoff.

IV. CONCLUSIONS

In this study, an attempt was made to provide a numerical description for the interplay between igniter, ullage, and bag material in a 155-mm artillery charge. Calculations were performed based on several

---

[24] *A.W. Horst, I.W. May, and E.V. Clarke, Jr., "The Missing Link Between Pressure Waves and Breechblows", ARBRL-MR-02849, USA ARRADCOM, Ballistic Research Laboratory, Aberdeen Proving Ground, MD, July 1978.* (AD#A058354)

limiting-case descriptions of the propellant bag. While assumptions concerning the behavior and influence of the bag were so crude as to prohibit one from describing the results as firm predictions of reality, several important conclusions can be drawn which impact on future model development and charge-design efforts alike.

First, the hydrodynamics of the ignition phase, as influenced by the subject parameters of this study, are shown to play a major role in determining whether or not propellant ignition will occur. Physically reasonable rates of igniter venting are not always sufficient for ignition, particularly if alternate paths of flow external to the propellant charge can equilibrate pressures and lower the pressure gradient into the bed. Increases in propellant surface temperature resulting from convective heating may then be sufficiently diminished by conduction into the grain that the ignition criterion is not met. It is interesting to note that further attempts to simulate long ignition delays by reapportioning the ignition output profile with respect to time (total igniter mass was held constant) were unsuccessful: either ignition was predicted to occur in a few milliseconds or not at all.

Moreover, a fully two-dimensional representation, by itself, is not expected to alter this aspect of the simulation in any substantive manner. An essential feature of the two-dimensional model must be an explicit representation of the flow resistance, strength, and burning properties of ignition system and propellant packaging materials. Ignition delays may be, in part, a result of the thermal destruction of such components. An improved simulation of the ignition event may await, as well, a more realistic criterion for propellant ignition, including recognition of a complicated sequence of events involved in transition to full combustion.

The above shortcomings of the present model, however, should not nullify the essential features of the subsequent phases of the solution. Once localized gas production is initiated, be it caused by igniter or propellant combustion, the path of flamespread may be significantly altered by bag material and configuration. The sensitivity of flamespread and ensuing pressure waves to bag permeability and rupture, particularly with forward ullage present, may offer a partial explanation for the variability in pressure waves observed in minimum-standoff M203 firings. Conversely, the occurrence of reproducible, high-amplitude pressure waves associated with maximum-standoff, M203 firings is consistent with the picture offered by both one-dimensional and quasi-two-dimensional descriptions: annular flow is of little consequence in terms of reducing pressure waves without the presence of forward ullage during flamespread.

Imbedded in this result lie some potentially significant implications with respect to the phenomenology of lower and multi-zone propelling charges. Annular ullage will remain very important to the control of pressure waves, but ignition transfer and separation characteristics

for multiple-increment packages may prove to be equally important. That same forward ullage which couples with annular ullage to provide an equilibration path for single-zone charges can also allow substantial propellant grain velocities to develop, a condition quite possibly exacerbated by the usual stacked, packaging configuration of multi-zone charges. Perhaps the increased degree of control over these parameters (as well as rupture strength and permeability) offered by rigid, combustible packaging materials will allow the future charge designer to provide the proper and consistent sequencing of flamespread and propellant motion to yield reproducibly low levels of pressure waves under all reasonable firing conditions.

V. FUTURE WORK

An effort is now underway to extend the current analysis to provide a fully two-dimensional representation of the problem. Our approach may be summarized as follows:

We divide the combustion chamber into disjoint regions in each of which all the flow variables may be regarded as continuously differentiable. In particular, one such region is allocated for each charge increment and the mixture boundaries always coincide with the region boundaries. Accordingly, a precise representation is made of the ullage. The flow inhibition associated with the bag material and its various liners may be embedded accurately as boundary conditions linking the flow in one region with that in its neighbors. For flexibility and economy we consider that the flow in a given region may be any one of two-dimensional, two-phase; two-dimensional, single-phase; quasi-one-dimensional, two-phase; quasi-one-dimensional, single-phase; or lumped-parameter, single-phase. The M203 Propelling Charge configuration is depicted within the framework of this representation in Figure 14.

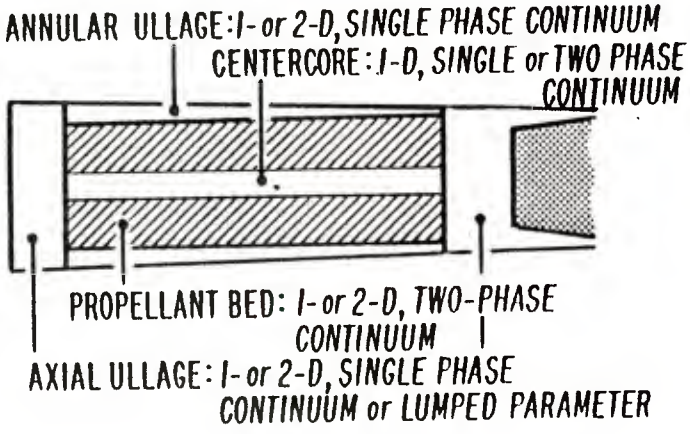

Figure 14. Two-Dimensional, Axisymmetric Representation

The governing equations for each of these types of regions consist of balance equations, which have been previously derived[6] and constitutive laws for which it is necessary, in some cases, to extrapolate from previous one-dimensional laws. The approach used to generate numerical solutions is essentially a marching technique based on an explicit two-step scheme. Each physical region is independently mapped, in a time-dependent manner, onto a regular computational figure, either a unit line or a unit square.

As a step towards the complete numerical implementation of the model, we have encoded a method of solution for a configurally complex, single region of two-dimensional, two-phase reacting flow in a closed chamber[7]. Stable solutions have been generated using this scheme for certain nominal data bases, and the extension of this code to treat initial ullage and the presence of the bag should lead to results to the current problem of interest by mid-1980.

REFERENCES

1. I.W. May and A.W. Horst, "Charge Design Considerations and Their Effect on Pressure Waves in Guns", Interior Ballistics of Guns, H. Krier and M. Summerfield, Editors, Progress in Astronautics and Aeronautics, Vol. 66, pp. 197-227, AIAA, New York, NY, 1979.

2. J. Chandra and C. Zoltani, Editors, Proceedings of ARO Workshop on Multiphase Flows, US Army Research Office, Research Triangle Park, NC, February 1978.

3. K.K. Kuo, "A Summary of the JANNAF Workshop on Theoretical Modeling and Experimental Measurements on the Combustion and Fluid Flow Processes in Gun Propellant Charges", 13th JANNAF Combustion Meeting, CPIA Publication 281, pp. 213-234, December 1976.

4. E.B. Fisher, "Quality Control of Continuously Produced Gun Propellant", Calspan Report No. SA-5913-X-1, Calspan Corporation, Buffalo, NY, August 1977.

5. E.B. Fisher, "Investigation of Breechblow Phenomenology", Calspan Report No. 1359-D-1, Calspan Corporation, Buffalo, NY, April 1979.

6. P.S. Gough and F.J. Zwarts, "Some Fundamental Aspects of the Digital Simulation of Convective Burning in Porous Beds:, AIAA Paper No. 77-855, AIAA/SAE 13th Propulsion Conference, July 1977.

7. P.S. Gough, "Theoretical Study of Two-Phase Flow Associated with Granular Bag Charges", ARBRL-CR-00381, USA ARRADCOM, Ballistic Research Laboratory, Aberdeen Proving Ground, MD, September 1978. (AD#A062144)

8. P.S. Gough, "Two Dimensional Convective Flamespreading in Packed Beds of Granular Propellant", ARBRL-CR-00404, USA ARRADCOM, Ballistic Research Laboratory, Aberdeen Proving Ground, MD, July 1979.(AD#A075326)

9. K.K. Kuo and J.H. Koo, "Transient Combustion in Granular Propellant Beds. Part 1: Theoretical Modeling and Numerical Solution of Transient Combustion Processes in Mobile Granular Propellant Beds", BRL-CR-346, USA ARRADCOM, Ballistic Research Laboratory, Aberdeen Proving Ground, MD, August 1977. (AD#A044998)

10. H. McDonald, "Two-Dimensional Implicit Interior Ballistics Code-Quarterly Technical Progress Report", Scientific Research Associates, Inc., November 1978.

11. A.C. Buckingham, "Research on Gun Barrel Erosion Mechanisms", Energy and Technology Review, Lawrence Livermore Laboratory, CA, January 1979.

12. A.W. Horst, T.C. Smith, and S.E. Mitchell, "Key Design Parameters in Controlling Gun-Environment Pressure Wave Phenomena - Theory Versus Experiment", 13th JANNAF Combustion Meeting, CPIA Publication 273, pp. 341-368, December 1975.

13. A.W. Horst and P.S. Gough, "Influence of Propellant Packaging on Performance of Navy Case Gun Ammunition", Journal of Ballistics, Vol. 1, No. 3, pp. 229-258, 1977.

14. C.W. Nelson, "Comparison of Predictions of Three Two-Phase Flow Codes", BRL-MR-2729, USA ARRADCOM, Ballistic Research Laboratory, Aberdeen Proving Ground, MD, February 1977.(AD#A037348)

15. A.W. Horst, C.W. Nelson, and I.W. May, "Flame Spreading in Granular Propellant Beds: A Diagnostic Comparison of Theory to Experiment", AIAA Paper No. 77-856, AIAA/SAE 13th Propulsion Conference, July 1977.

16. E.B. Fisher and A.P. Trippe, "Development of a Basis for Acceptance of Continuously Produced Propellant", Calspan Report No. VQ-5163-D-1, Calspan Corporation, Buffalo, NY, November 1973.

17. C.K. Zoltani, "M-82 Primer Flow Study", ARBRL-TR-02084, USA ARRADCOM, Ballistic Research Laboratory, Aberdeen Proving Ground, MD, June 1978. (AD#A057695)

18. S. Ergun, "Fluid Flow Through Packed Columns", Chem. Eng. Progr., Vol 48, pp. 89-95, 1952.

19. K.E.B. Andersson, "Pressure Drop in Ideal Fluidization", Chem. Eng. Sci., Vol. 15, pp. 276-297, 1961.

20. W.H. Denton, "General Discussion on Heat Transfer", Inst. Mech Eng. and Am. Soc. Mech. Eng., London, 1951.

21. N.I. Gelperin and V.G. Einstein, "Heat Transfer in Fluidized Beds", Fluidization, J.F. Davidson and D. Harrison, Editors, Academic Press, 1971.

22. R.W. MacCormack, "The Effects of Viscosity in Hypervelocity Impact Cratering", AIAA Paper No. 69-354, AIAA 7th Aerospace Science Meeting, 1969.

23. A.W. Horst and T.R. Trafton, "NOVA Code Simulation of a 155-mm Howitzer: An Update", ARBRL-MR-02967, USA ARRADCOM, Ballistic Research Laboratory, Aberdeen Proving Ground, MD, October 1979.(AD#A079893)

24. A.W. Horst, I.W. May, and E.V. Clarke, Jr., "The Missing Link Between Pressure Waves and Breechblows", ARBRL-MR-02849, USA ARRADCOM, Ballistic Research Laboratory, Aberdeen Proving Ground, MD, July 1978. (AD#A058354)

APPENDIX A.

INPUT DATA FOR QUASI-ONE-DIMENSIONAL SIMULATIONS

155MM,M203,M199,M483 MIN SD,1D IG SIM

CONTROL DATA

LOGICAL VARIABLES:
PRINT 1 GRAPH 2 DISK WRITE 0 DISK READ 0
I.B. TABLE 1 FLAME TABLE 1 PRESSURE TABLE(S) 1
EROSIVE EFFECT 0 DYNAMIC EFFECT 0 WALL TEMPERATURE CALCULATION 0
LEFT HAND BOUNDARY CONDITION 0 RIGHT HAND BOUNDARY CONDITION 0 LEFT HAND RESERVOIR 0
RIGHT HAND RESERVOIR 0 BED PRECOMPRESSED 0
HEAT LOSS CALCULATION 0 INSULATING LAYER 0

BORE RESISTANCE FUNCTION 1

INTEGRATION PARAMETERS

NUMBER OF STATIONS AT WHICH DATA ARE STORED	30
NUMBER OF STEPS BEFORE LOGOUT	100
TIME STEP FOR DISK START	0
NUMBER OF STEPS FOR TERMINATION	2500
TIME FOR TERMINATION (SEC)	.5000E-01
PROJECTILE TRAVEL FOR TERMINATION (INS)	205.00
MAXIMUM TIME STEP (SEC)	.1000E-03
STABILITY SAFETY FACTOR	2.00
SOURCE STABILITY FACTOR	.0500
SPATIAL RESOLUTION FACTOR	.0100
TIME INTERVAL FOR I.B. TABLE STORAGE(SEC)	.2000E-03
TIME INTERVAL FOR PRESSURE TABLE STORAGE (SEC)	.1000E-03

FILE COUNTERS

NUMBER OF STATIONS TO SPECIFY TUBE RADIUS	7
NUMBER OF TIMES TO SPECIFY PRIMER DISCHARGE	8
NUMBER OF POSITIONS TO SPECIFY PRIMER DISCHARGE	5
NUMBER OF ENTRIES IN BORE RESISTANCE TABLE	7
NUMBER OF ENTRIES IN WALL TEMPERATURE TABLE	0
NUMBER OF ENTRIES IN FILLER ELEMENT TABLE	0
NUMBER OF TYPES OF PROPELLANTS	1
NUMBER OF BURN RATE DATA SETS	2
NUMBER OF ENTRIES IN VOID FRACTION TABLE(S)	0 0 0
NUMBER OF ENTRIES IN PRESSURE HISTORY TABLES	3
NUMBER OF ENTRIES IN LEFT BOUNDARY SOURCE TABLE	0
NUMBER OF ENTRIES IN RIGHT BOUNDARY SOURCE TABLE	0
NUMBER OF WALL STATIONS FOR INVARIANT EMBEDDING	0
NUMBER OF BED STATIONS FOR INVARIANT EMBEDDING	0
FRICTION COEFFICIENT	1.0

GENERAL PROPERTIES OF INITIAL AMBIENT GAS

INITIAL TEMPERATURE (DEG.R)	530.0
INITIAL PRESSURE (PSI)	14.7
MOLECULAR WEIGHT (LBM/LBMOL)	29.000
RATIO OF SPECIFIC HEATS	1.4000

GENERAL PROPERTIES OF PROPELLANT BED

INITIAL TEMPERATURE (DEG.R)	530.0
VIRTUAL MASS CONSTANT (-)	0.000
VOID FRACTION PACKING COEFFICIENTS	0.0000 0.0000 0.0000

PROPERTIES OF PROPELLANT 1

PROPELLANT TYPE	M30A1+RAD-E-069805
MASS OF PROPELLANT (LBM)	26.1500
DENSITY OF PROPELLANT (LBM/IN**3)	.0572
FORM FUNCTION INDICATOR	7
OUTSIDE DIAMETER (INS)	.4173
INSIDE DIAMETER (INS)	.0338
LENGTH (INS)	.9481
NUMBER OF PERFORATIONS	7.

RHEOLOGICAL PROPERTIES

SPEED OF COMPRESSION WAVE IN SETTLED BED (IN/SEC)	6000.
SETTLING POROSITY	.4243
SPEED OF EXPANSION WAVE (IN/SEC)	50000.

SOLID PHASE THERMOCHEMISTRY

MAXIMUM PRESSURE FOR BURN RATE DATA (LBF/IN**2)	10000.
BURNING RATE PRE-EXPONENTIAL FACTOR (IN/SEC/PSI**BN)	.6918E-02
BURNING RATE EXPONENT	.6337
MAXIMUM PRESSURE FOR BURN RATE DATA (LBF/IN**2)	60000.
BURNING RATE PRE-EXPONENTIAL FACTOR (IN/SEC/PSI**BN)	.1743E-02
BURNING RATE EXPONENT	.7864
BURNING RATE CONSTANT (IN/SEC)	0.0000
IGNITION TEMPERATURE (DEG.R)	800.0
ARRHENIUS ACTIVATION ENERGY (LBF-IN/LBMOL)	0.
FREQUENCY FACTOR (SEC**-1)	0.
THERMAL CONDUCTIVITY (LBF/SEC/DEG.R)	.2770E-01
THERMAL DIFFUSIVITY (IN**2/SEC)	.1345E-03
EMISSIVITY FACTOR	.660

GAS PHASE THERMOCHEMISTRY

CHEMICAL ENERGY RELEASED IN BURNING(LBF-IN/LBM)	.17600E+08
MOLECULAR WEIGHT (LBM/LBMOL)	23.3600
RATIO OF SPECIFIC HEATS	1.2430
COVOLUME	28.5000

LOCATION OF PACKAGE(S)

PACKAGE	LEFT BODY(INS)	RIGHT BODY(INS)	MASS(LBM)
1	1.000	31.000	26.150

PROPERTIES OF PRIMER

CHEMICAL ENERGY RELEASED IN BURNING(LBF-IN/LBM)	.6303E+07
MOLECULAR WEIGHT (LBM/LBMOL)	36.1300
RATIO OF SPECIFIC HEATS	1.2500
SPECIFIC VOLUME OF SOLID(IN**3/LBM)	15.3850

PRIMER DISCHARGE FUNCTION (LBM/IN/SEC)

POS.(INS) TIME(SEC)	0.00	.98	.99	30.00	31.00
0.	3.00	3.00	0.00	0.00	0.00
.100E-01	3.00	3.00	0.00	0.00	0.00
.110E-01	0.00	0.00	0.00	0.00	0.00
.490E-01	0.00	0.00	0.00	0.00	0.00
.500E-01	0.00	1.00	1.00	1.00	0.00
.600E-01	0.00	1.00	1.00	1.00	0.00
.610E-01	0.00	0.00	0.00	0.00	0.00
.100E+00	0.00	0.00	0.00	0.00	0.00

PARAMETERS TO SPECIFY TUBE GEOMETRY

DISTANCE(IN)	RADIUS(IN)
0.000	3.330
1.345	3.324
1.345	3.402
17.630	3.250
36.409	3.165
38.796	3.080
240.000	3.080

BORE RESISTANCE TABLE

POSITION(INS)	RESISTANCE(PSI)
35.000	250.
35.400	3350.
36.000	4950.
36.550	3625.
37.050	3250.
39.500	2500.
240.000	1500.

THERMAL PROPERTIES OF TUBE

THERMAL CONDUCTIVITY (LBF/SEC/DEG.R)	7.770
THERMAL DIFFUSIVITY (IN**2/SEC)	.2280E-01
EMISSIVITY FACTOR	.700
INITIAL TEMPERATURE (DEG.R)	530.00

PROJECTILE AND RIFLING DATA

INITIAL POSITION OF BASE OF PROJECTILE(INS)	35.000
MASS OF PROJECTILE (LBM)	103.000
POLAR MOMENT OF INERTIA (LBM-IN**2)	14.000
ANGLE OF RIFLING (DEG)	6.000

POSITIONS FOR PRESSURE TABLE STORAGE

0.0000 16.0000 32.0000

APPENDIX B.

INPUT DATA FOR QUASI-TWO-DIMENSIONAL SIMULATIONS

M203,M199,M483 MIN SO,WEAK PERM BAG

LOCATION OF PACKAGE(S)

PACKAGE	LEFT BODY(INS)	RIGHT BODY(INS)	MASS(LBM)
1	1.000	31.000	26.150

RADIUS OF BAG (INS) 2.900
RUPTURE PRESSURE OF BAG (PSI) 0.000
MASS TRANSFER FACTOR (-) 1.000
AREA FACTOR (-) .5000E-01
ICL ARRAY 1111111111111111111111111111111

INITIAL BAG STRENGTH ARRAY

0.	0.	0.	0.	0.
0.	0.	0.	0.	0.
0.	0.	0.	0.	0.
0.	0.	0.	0.	0.
0.	0.	0.	0.	0.
0.	0.	0.	0.	0.
0.				

M203,M199,M483 MAX SO,WEAK PERM BAG

LOCATION OF PACKAGE(S)

PACKAGE	LEFT BODY(INS)	RIGHT BODY(INS)	MASS(LBM)
1	5.000	35.000	26.150

RADIUS OF BAG (INS) 2.900
RUPTURE PRESSURE OF BAG (PSI) 0.000
MASS TRANSFER FACTOR (-) 1.000
AREA FACTOR (-) .5000E-01
ICL ARRAY 1111111111111111111111111111111

INITIAL BAG STRENGTH ARRAY

0.	0.	0.	0.	0.
0.	0.	0.	0.	0.
0.	0.	0.	0.	0.
0.	0.	0.	0.	0.
0.	0.	0.	0.	0.
0.	0.	0.	0.	0.
0.				

M203,M199,M483 - IN SO,STRONG IMPERM BAG

LOCATION OF PACKAGE(S)

PACKAGE	LEFT BODY(INS)	RIGHT BODY(INS)	MASS(LBM)
1	1.000	31.000	27.150

RADIUS OF BAG (INS) 2.900
RUPTURE PRESSURE OF BAG (PSI) -1000.000
MASS TRANSFER FACTOR (-) 1.000
AREA FACTOR (-) .5000E-01
ICL ARRAY 00000000000000000000000000000

INITIAL BAG STRENGTH ARRAY

.10000E+04	.10000E+04	.10000E+04	.10000E+04	.10000E+04
.10000E+04	.10000E+04	.10000E+04	.10000E+04	.10000E+04
.10000E+04	.10000E+04	.10000E+04	.10000E+04	.10000E+04
.10000E+04	.10000E+04	.10000E+04	.10000E+04	.10000E+04
.10000E+04	.10000E+04	.10000E+04	.10000E+04	.10000E+04
.10000E+04	.10000E+04	.10000E+04	.10000E+04	.10000E+04
0.				

M203,M199,M483 MAX SO,STRONG IMPERM BAG

LOCATION OF PACKAGE(S)

PACKAGE	LEFT BODY(INS)	RIGHT BODY(INS)	MASS(LBM)
1	5.000	35.000	26.150

RADIUS OF BAG (INS) 2.900
RUPTURE PRESSURE OF BAG (PSI) **********
MASS TRANSFER FACTOR (-) 1.000
AREA FACTOR (-) .5000E-01
ICL ARRAY 00000000000000000000000000000

INITIAL BAG STRENGTH ARRAY

.10000E+06	.10000E+06	.10000E+06	.10000E+06	.10000E+06
.10000E+06	.10000E+06	.10000E+06	.10000E+06	.10000E+06
.10000E+06	.10000E+06	.10000E+06	.10000E+06	.10000E+06
.10000E+06	.10000E+06	.10000E+06	.10000E+06	.10000E+06
.10000E+06	.10000E+06	.10000E+06	.10000E+06	.10000E+06
.10000E+06	.10000E+06	.10000E+06	.10000E+06	.10000E+06
0.				

M203,M199,M483 MIN SO, STR PERM BAG

LOCATION OF PACKAGE(S)

PACKAGE	LEFT BODY(INS)	RIGHT BODY(INS)	MASS(LBM)
1	1.000	31.000	26.150

RADIUS OF BAG (INS) 2.900
RUPTURE PRESSURE OF BAG (PSI) -1000.000
MASS TRANSFER FACTOR (-) 1.000
AREA FACTOR (-) .5000E-01
ICL ARRAY 1111111111111111111111111111111

INITIAL BAG STRENGTH ARRAY

.10000E+04	.10000E+04	.10000E+04	.10000E+04	.10000E+04
.10000E+04	.10000E+04	.10000E+04	.10000E+04	.10000E+04
.10000E+04	.10000E+04	.10000E+04	.10000E+04	.10000E+04
.10000E+04	.10000E+04	.10000E+04	.10000E+04	.10000E+04
.10000E+04	.10000E+04	.10000E+04	.10000E+04	.10000E+04
.10000E+04	.10000E+04	.10000E+04	.10000E+04	.10000E+04
0.				

M203,M199,M483 MAX SO, STR PERM BAG

LOCATION OF PACKAGE(S)

PACKAGE	LEFT BODY(INS)	RIGHT BODY(INS)	MASS(LBM)
1	5.000	35.000	26.150

RADIUS OF BAG (INS) 2.900
RUPTURE PRESSURE OF BAG (PSI) -1000.000
MASS TRANSFER FACTOR (-) 1.000
AREA FACTOR (-) .5000E-01
ICL ARRAY 1111111111111111111111111111111

INITIAL BAG STRENGTH ARRAY

.10000E+04	.10000E+04	.10000E+04	.10000E+04	.10000E+04
.10000E+04	.10000E+04	.10000E+04	.10000E+04	.10000E+04
.10000E+04	.10000E+04	.10000E+04	.10000E+04	.10000E+04
.10000E+04	.10000E+04	.10000E+04	.10000E+04	.10000E+04
.10000E+04	.10000E+04	.10000E+04	.10000E+04	.10000E+04
.10000E+04	.10000E+04	.10000E+04	.10000E+04	.10000E+04
0.				

DISTRIBUTION LIST

No. of Copies	Organization
12	Commander Defense Technical Info Center ATTN: DDC-DDA Cameron Station Alexandria, VA 22314
1	Director Defense Advanced Research Projects Agency ATTN: E.F. Blase 1400 Wilson Boulevard Arlington, VA 22209
1	Director Institute for Defense Analyses ATTN: R.C. Oliver 400 Army-Navy Drive Arlington, VA 22202
1	Commander US Army Materiel Development & Readiness Command ATTN: DRCDMD-ST 5001 Eisenhower Avenue Alexandria, VA 22333
1	Commander US Army Materiel Development & Readiness Command ATTN: DRCDE-DW, S.R. Matos 5001 Eisenhower Avenue Alexandria, VA 22333
5	Commander US Army Armament Research & Development Command ATTN: DRDAR-TSS (2 cys) DRDAR-LCE, R. Walker C. Lenchitz DRDAR-SCA, L. Stiefel Dover, NJ 07801
5	Commander US Army Armament Research & Development Command ATTN: DRDAR-LCA, H. Fair E. Wurzel S. Bernstein S. Einstein P. Kemmey Dover, NJ 07801
1	Commander US Army Armament Materiel Readiness Command ATTN: DRDAR-LEP-L, Tech Lib Rock Island, IL 61299
1	Director US Army ARRADCOM Benet Weapons Laboratory ATTN: DRDAR-LCB-TL Watervliet, NY 12189
1	Commander US Army Watervliet Arsenal ATTN: SARWV-RD, R. Thierry Watervliet, NY 12189
1	Commander US Army Aviation Research & Development Command ATTN: DRSAV-E P.O. Box 209 St. Louis, MO 63166
1	Director US Army Air Mobility Research & Development Laboratory Ames Research Center Moffett Field, CA 94035
1	Commander US Army Communications Research & Development Command ATTN: DRDCO-PPA-SA Fort Monmouth, NJ 07703

DISTRIBUTION LIST

No. of Copies	Organization
1	Commander US Army Eelctronics Research & Development Command Technical Support Activity ATTN: DELSD-L Fort Monmouth, NJ 07703
1	Commander US Army Missile Command ATTN: DRSMI-R Redstone Arsenal, AL 35809
1	Commander US Army Missile Command ATTN: DRSMI-YDL Redstone Arsenal, AL 35809
1	Commander US Army Missile Command ATTN: DRDMI-RK, R.G. Rhoades Redstone Arsenal, AL 35809
1	Commander US Army Tank Automotive Research & Development Command ATTN: DRDTA-UL Warren, MI 48090
1	Commander US Army Materials and Mechanics Research Center ATTN: DRXMR-ATL Watertown, MA 02172
1	Commander US Army Natick Research & Development Command ATTN: DRXRE, D. Sieling Natick, MA 01762
1	Commander US Army Research Office ATTN: Tech Lib P.O. Box 12211 Research Triangle Park, NC 27706
1	Director US Army TRADOC Systems Analysis Activity ATTN: ATAA-SL, Tech Lib White Sands Missile Range NM 88002
1	Chief of Naval Research ATTN: Code 473, R.S. Miller 800 N. Quincy Street Arlington, VA 22217
1	Commander Naval Sea Systems Command ATTN: SEA-62R2, J.W. Murrin Washington, DC 20362
2	Commander Naval Surface Weapons Center ATTN: Code G33, J.L. East Code DX-21, Tech Lib Dahlgren, VA 22448
1	Commander Naval Surface Weapons Center ATTN: Code 240, S.J. Jacobs Code 730 Silver Spring, MD 20910
1	Commanding Officer Naval Underwater Systems Center Energy Conversion Dept. ATTN: Code 5B331, R.S. Lazar Newport, RI 02840
2	Commander Naval Weapons Center ATTN: Code 388, R.L. Derr C.F. Price China Lake, CA 93555
1	Superintendent Naval Postgraduate School Dept of Mechanical Engineering ATTN: A.E. Fuhs Monterey, CA 93940

DISTRIBUTION LIST

No. of Copies	Organization
2	Commander Naval Ordnance Station ATTN: P.L. Stang F.W. Robbins Indian Head, MD 20640
2	AFRPL/DYSC (D.George,J.N.Levine) Edwards, AFB, CA 93523
1	AFATL/DLDL (O.K.Heiney) Eglin AFB, FL 32542
1	Lawrence Livermore Laboratory ATTN: MS L-355, A. Buckingham P.O. Box 808 Livermore, CA 94550
1	Aerojet Solid Propulsion Co. ATTN: P. Micheli Sacramento, CA 95813
1	ARO Incorporated ATTN: N. Dougherty Arnold AFS, TN 37389
1	Atlantic Research Corporation ATTN: M.K. King 5390 Cherokee Avenue Alexandria, VA 22314
1	AVCO Corporation AVCO Everett Research Lab Div ATTN: D. Stickler 2385 Revere Beach Parkway Everett, MA 02149
1	Calspan Corporation ATTN: E.B. Fisher P.O. Box 400 Buffalo, NY 14221
1	Foster Miller Associates, Inc. ATTN: A.J. Erickson 135 Second Avenue Waltham, MA 02154
1	General Applied Sciences Labs ATTN: J. Erdos Merrick & Stewart Avenues Westbury Long Island, NY 11590
1	General Electric Company Armament Systems Dept. ATTN: M.J. Bulman, Rm. 1311 Lakeside Avenue Burlington, VT 05402
1	Hercules, Inc. Allegany Ballistics Laboratory ATTN: R.B. Miller P.O. Box 210 Cumberland, MD 21502
1	Hercules, Inc. Bacchus Works ATTN: K.P. McCarty P.O. Box 98 Magna, UT 84044
1	Hercules, Inc. Eglin Operations ATTN: R.L. Simmons Eglin AFB, FL 32542
1	Olin Corporation Badger Army Ammunition Plant ATTN: R.J. Thiede Baraboo, WI 53913
1	Olin Corporation Smokeless Powder Operations ATTN: R.L. Cook P.O. Box 222 St. Marks, FL 32355
1	Paul Gough Associates, Inc. ATTN: P.S. Gough P.O. Box 1614 Portsmouth, NH 03801
1	Physics International Company 2700 Merced Street Leandro, CA 94577

DISTRIBUTION LIST

No. of Copies	Organization
1	Pulsepower Systems, Inc. ATTN: L.C. Elmore 815 American Street San Carlos, CA 94070
1	Rockwell International Corp. Rocketdyne Division ATTN: BA08, J.E. Flanagan 6633 Canoga Avenue Canoga Park, CA 91304
1	Science Applications, Inc. ATTN: R.B. Edelman 32146 Cumorah Crest Woodland Hills, CA 91364
1	Scientific Research Assoc., Inc. ATTN: H. McDonald P.O. Box 498 Glastonbury, CT 06033
1	Shock Hydrodynamics, Inc. ATTN: W.H. Anderson 4710-16 Vineland Avenue North Hollywood, CA 91602
3	Thiokol Corporation Huntsville Division ATTN: D. Flanigan R. Glick Tech Lib Huntsville, AL 35807
2	Thiokol Corporation Wasatch Division ATTN: John Peterson Tech Lib P.O. Box 524 Brigham City, UT 84302
2	Chemical Systems Div United Technologies ATTN: R. Brown Tech Lib P.O. Box 358 Sunnyvale, CA 94086
1	Universal Propulsion Company ATTN: H.J. McSpadden 1800 W. Deer Valley Rd Phoenix, AZ 85027
1	Battelle Memorial Institute ATTN: Tech Lib 505 King Avenue Columbus, OH 43201
1	Brigham Young University Dept of Chemical Engineering ATTN: Dr. M. Beckstead Provo, UT 84601
1	California Institute of Tech 204 Karman Lab Mail Stop 301-46 ATTN: F.E.C. Culick 1201 E. California Street Pasadena, CA 91125
1	California Institute of Technology Jet Propulsion Laboratory ATTN: L.D. Strand 4800 Oak Grove Drive Pasadena, CA 91103
1	Case Western Reserve University Division of Aerospace Sciences ATTN: J. Tien Cleveland, OH 44135
3	Georgia Institute of Tech School of Aerospace Eng. ATTN: B.T. Zinn E. Price W.C. Strahle Atlanta, GA 30332
1	IIT Research Institute ATTN: M.J. Klein 10 W. 35th Street Chicago, IL 60616

DISTRIBUTION LIST

No. of Copies	Organization
1	Institute of Gas Technology ATTN: D. Gidaspow 3424 S. State Street Chicago, IL 60616
1	Johns Hopkins University Applied Physics Laboratory Chemical Propulsion Information Agency ATTN: T. Christian Johns Hopkins Road Laurel, MD 20810
1	Massachusetts Institute of Technology Dept of Mechanical Engineering ATTN: T. Toong Cambridge, MA 02139
1	Pennsylvania State University Applied Research Lab ATTN: G.M. Faeth P.O. Box 30 State College, PA 16801
1	Pennsylvania State University Dept of Mechanical Engineering ATTN: K. Kuo University Park, PA 16802
1	Princeton University Forrestal Campus Library ATTN: L.H. Caveny P.O. Box 710 Princeton, NJ 08544
1	Purdue University School of Mechanical Engineering ATTN: J.R. Osborn TSPC Chaffee Hall West Lafayette, IN 47907
1	Rensselaer Polytechnic Inst. Department of Mathematics ATTN: Prof. D.A. Drew Troy, NY 12181
1	Rutgers State University Dept of Mechanical and Aerospace Engineering ATTN: S. Temkin University Heights Campus New Brunswick, NJ 08903
1	SRI International Propulsion Sciences Division ATTN: Tech Lib 333 Ravenswood Avenue Menlo Park, CA 94024
1	Stevens Institute of Technology Davidson Laboratory ATTN: R. McAlevy, III Hoboken, NJ 07030
1	University of California Los Alamos Scientific Lab ATTN: T3, D. Butler P.O. Box 1663 Los Alamos, NM 87545
1	University of California San Diego AMES Department ATTN: F.A. Williams P.O. Box 109 La Jolla, CA 92037
1	University of Southern California Mechanical Engineering Dept. ATTN: OHE200, M. Gerstein Los Angeles, CA 90007
1	University of Illinois AAE Department ATTN: H. Krier Transportation Bldg. Rm 105 Urbana, IL 61801
1	University of Massachusetts Dept of Mechanical Engineering ATTN: K. Jakus Amherst, MA 01002

DISTRIBUTION LIST

No. of Copies	Organization
1	University of Minnesota Dept of Mechanical Engineering ATTN: E. Fletcher Minneapolis, MN 55455
2	University of Utah Dept of Chemical Engineering ATTN: A. Baer G. Flandro Salt Lake City, UT 84112
1	Washington State University Dept of Mechanical Engineering ATTN: Prof. C.T. Crowe Pullman, WA 99163

No. of Copies	Organization
	Aberdeen Proving Ground
	Dir, USAMSAA ATTN: DRXSY-D DRXSY-MP, H. Cohen
	Cdr, USATECOM ATTN: DRSTE-TO-F
	Dir, CSL Bldg E3516, EA ATTN: DRDAR-CLB-PA

USER EVALUATION OF REPORT

Please take a few minutes to answer the questions below; tear out this sheet and return it to Director, US Army Ballistic Research Laboratory, ARRADCOM, ATTN: DRDAR-TSB, Aberdeen Proving Ground, Maryland 21005. Your comments will provide us with information for improving future reports.

1. BRL Report Number _____

2. Does this report satisfy a need? (Comment on purpose, related project, or other area of interest for which report will be used.)

_____

_____

_____

3. How, specifically, is the report being used? (Information source, design data or procedure, management procedure, source of ideas, etc.) _____

_____

_____

4. Has the information in this report led to any quantitative savings as far as man-hours/contract dollars saved, operating costs avoided, efficiencies achieved, etc.? If so, please elaborate.

_____

_____

5. General Comments (Indicate what you think should be changed to make this report and future reports of this type more responsive to your needs, more usable, improve readability, etc.) _____

_____

_____

_____

6. If you would like to be contacted by the personnel who prepared this report to raise specific questions or discuss the topic, please fill in the following information.

Name: _____

Telephone Number: _____

Organization Address: _____

_____

_____